Studying the physics beyond the Standard Model in rare semileptonic $B \to K^* \mu^+ \mu^-$ decays with the ATLAS detector

D. Melikhov, N. Nikitin, F. Rizatdinova and L. Smirnova
Moscow State University, Nuclear Physics Institute, Moscow, 119899, Russia

We discuss a possibility to disentangle the new physics effects by analyzing the leptonic forward-backward asymmetry in rare semileptonic $B \to K^* \mu^+ \mu^-$ decays. This asymmetry is largely unaffected by the uncertainties in the long-distance (LD) contributions to the $B \to K^* \mu^+ \mu^-$ amplitude, and at the same time is sensitive to the short-distance (SD) Wilson coefficients which encode the information on the structure of the theory at large mass scales and thus are different, e.g., in the Standard Model and its extentions. We demonstrate that the application of the kinematical cuts of the ATLAS detector at LHC preserves this sensitivity of the asymmetry to the short-distance effects and thus allows one to experimentally test the SM and its extentions.

1. Introduction

Rare semileptonic B–decays induced by b–quark transition $b \to (s,d) l^+ l^-$ provide an impotant test of the Standard Model (SM) and its possible extentions. These transitions are caused by Flavor Changing Neutral Currents (FCNC) which forbidden at the tree level in the SM [1] and therefore have very small probabilities of $10^{-5} - 10^{-11}$. The FCNC transitions proceed in the leading order through the one-loop diagrams. This fact opens a possibility to probe at comparatively low energies the structure of the electroweak theory at large mass scales, due to the contributions of virtual particles in the loops. Moreover, these transitions are expected to be sensitive to possible new interactions, provided by the extentions of the SM. Thus an experimental study of such decays open a window on physics beyond the SM. In this paper we consider the case of exclusive $b \to s l^+ l^-$ decay modes. The effective Hamiltonian which governs the $b \to s l^+ l^-$ transition in the limit $m_s = 0$ has the following structure [2]:

$$\mathcal{H}_{eff}(b \to s l^+ l^-) = \frac{G_F}{\sqrt{2}} \frac{\alpha_{em}}{2\pi} V_{ts}^* V_{tb} \left[-2i \frac{m_b}{q^2} C_{7\gamma}(\mu) (\bar{s} \sigma_{\mu\nu} q^\nu (1+\gamma_5) b)(\bar{l} \gamma^\mu l) + \right. \tag{1}$$
$$\left. C_{9V}^{eff}(\mu, q^2)(\bar{s}\gamma_\mu(1-\gamma_5)b)(\bar{l}\gamma^\mu l) + C_{10A}(\mu)(\bar{s}\gamma_\mu(1-\gamma_5)b)(\bar{l}\gamma^\mu\gamma_5 l) \right].$$

Here q^2 is the invariant mass squared of the lepton pair and $C_i(\mu)$ are the Wilson coefficients which encode the information on the short-distance dynamics of the theory. The parameter μ in the equation (1) is a typical scale which separates the long and short distances. For B decays it is convenient to choose this scale $\mu \sim m_b$. The amplitude of the $B \to K^* l^+ l^-$ decay is obtained by taking the matrix element of the effective Hamiltonian between the B and K^* states. The contribution of the long-distance effects which are responsible for the meson formation in the initial and final states are encoded in the $B \to K^*$ transition form factors which appear as invariant structures in the Lorentz decomposition of the corresponding amplitude. These form factors should be calculated on the basis of a nonperturbative treatment and provide the main source of uncertainties in the theoretical consideration of exclusive decays. It is known (see, e.g. [3] and refs therein) that these form factors are rather strongly dependent on the details of the model used for the description of the long-distance effects and this model-dependence yields considerable uncertainties in the predictions of the decay rates and dilepton distributions within the SM. This dependence of the theoretical predictions for the decay rates on the uncertainty in the hadronic transition form factors considerably complicates a study of the new physics effects encoded in the Wilson coefficients, since in most of the observables the LD and SD effects act coherently. Fortunately, as it was discussed in [3], e.g. the forward-backward lepton asymmetry remains rather stable with respect to the obtained uncertainties in the form factors, but at the same time demonstrates sensitivity to the Wilson coefficients. Thus experimental study of the forward-backward asymmetry opens a possibility to 'measure' the Wilson coefficients and thus to test the SM and its extentions.

In this paper we demonstrate that it is possible to obtain sufficiently accurate measurements of the asymmetries with the ATLAS detector after the 3 year run at low luminosity and thus to obtain an important information on the values of the Wilson coefficients.

2. Theoretical predictions for the $B \to K(K^*)\mu^+\mu^-$ decays in the SM

Table I presents theoretical predictions for the branching ratios of the $B \to K\mu^+\mu^-$ and $B \to K^*\mu^+\mu^-$ decays obtained with two sets of transition form factors from ref [3]. These two sets of the form factors are obtained within the relativistic quark model using different quark model parameters, and the difference between them reflects the typical uncertainty in our knowledge of the LD effects. We also list in this Table the results obtained by Ali [5] using the heavy quark symmetry relations for the form factors. The average values turn out to be in good agreement, but the typical spread of predictions is rather large *. Because of such drastic uncertainty in our present knowledge of the LD effects, there is no way to study a new physics effects by the analysis of the decay rates or the dilepton q^2-distributions.

A favourable possibility was proposed in [3] where it was noticed that the forward-backward lepton asymmetry remains largely unaffected by the uncertainty in the transition form factors but is mostly determined by the value of the Wilson coefficient $C_7\gamma$ in the SM (Fig. 1). Moreover, the shape of the A_{FB} is rather sensitive to the variations of this Wilson coefficient.

A window for the allowed values of $C_{7\gamma}$ is provided by the CLEO results on the rare radiative: namely, the quantity $R_{7\gamma} = C_{7\gamma}(M_W)/C_{7\gamma}^{SM}(M_W)$ lies in one of the following intervals

$$-4.2 < R_{7\gamma} < -2.4, \qquad 0.4 < R_{7\gamma} < 1.2. \tag{2}$$

For example, there are regions in the Minimal Supersymmetric Model (MSSM) parameter space which yield the negative values of $R_{7\gamma}$ [7]. As shown in Fig. 1, the shape of the forward-backward asymmetry turns out to be qualitatively different for positive and negative values of $R_{7\gamma}$. Thus, in principle, an experimental study of this asymmetry allows one to obtain information on the value of the Wilson coefficient $C_{7\gamma}$. Apriory, it is not clear however whether the abovementioned sensitivity of the foward-backward asymmetry to the SD effects encoded in the Wilson coefficients holds or not after applying the kinematical cuts implemented in the ATLAS detector at LHC. In the next section we analyze the sensitivity of the experimentally measured dilepton distributions to the variations in the transition form factors and the sensitivity of the experimentally measured asymmetries to the Wilson coefficient.

An important conclusion is that the sensitivity of the forward-backward asymmetry to the value of the Wilson coefficient does take place after the cuts and thus it is really possible to test the SM in the exclusive $B \to K^*l^+l^-$ decays.

3. Studying the muon distributions with ATLAS

First, we study the sensitivity of the experimantally observed characteristics of the $B_d^0 \to K^{*0}\mu^+\mu^-$ decays to the uncertainty in the transition form factors. To this end, 3 sets of signal events have been generated with PYTHIA. The first set of events was generated using the standard PYTHIA matrix element for decay of B-meson. The second and third samples were generated using the two sets of the transition

The particle parameters were smeared according to the expected experimental resolution. The probability to identify a muon was assumed to be $\epsilon_\mu = 0.8$ [6].

In the Fig. 2 (a,b) the distributions of the largest p_T of muon and p_T–distribution of second muon are shown for the 3 sets of events. The corresponding average values $p^\mu_{T\,min}$ and $p^\mu_{T\,max}$ for three samples are presented in Table II. One can see from the spectra and average values that muon p_T–distributions in rare semileptonic B–decay are not sensitive to the q^2–dependence of matrix element. So, deviations of the muon p_T-distribution from the predicted by SM one can be considered as the indication of physics beyond SM.

Due to the absence of any dependence of p_T–muon spectra on the matrix elements we expect that the sharp cuts on p_T of muons (caused by the trigger requirements and muon identification) will not reduce the expected cross-section of $B_d^0 \to K^{*0}\mu^+\mu^-$ signal stronger than it was found in our previous studies [6].

The similarity of muon parameters means that kinematics of the decays is practically the same. It is demonstrated by the results in Table III, where the sensitivity of signal event samples to cuts is shown

*Notice that the present results turn out to be a factor 2 smaller then the results of an earlier analysis of Ref. [4], which have been used in our previous estimates for ATLAS [6].

with corresponding cross-sections of background events. The cuts are proposed in [6] and are the following (see also Table III):

1) The decay lengths of the reconstructed B_d^0 and K^{*0} were required to be more than 1 mm and χ^2 per number of degrees of freedom of the reconstructed B_d^0 vertex was required to be smaller than 3. This cut is expected to be effective in suppressing tracks from the primary vertex and Drell-Yan pairs.

2) Angle between the vector directed from primary vertex to the vertex of B_d^0 decay and the vector of B_d^0's transverse momentum $\alpha < 3°$. This cut suppresses the background combinations in the case where particles are from different jets.

3) Requirement of absence of charged particles with $p_T > 1$ GeV/c in the cone $< 9°$ around the B-direction. This cut suppresses background combinations from two b-quarks produced by a gluon splitting.

4) The effective dimuon mass should be out of the J/ψ and ψ' mass regions. To exclude the muons from J/ψ, the mass region $3.009 < M_{\mu\mu}^{eff} < 3.185$, corresponding to ± 5 standard deviations of the J/ψ-mass with ATLAS resolution, was rejected. The muons within ± 100 MeV/c^2 around the average ψ'-mass were also excluded.

5) The transverse momentum of the K^{*0} should be greater than 5 GeV/c.

The probabilities to pass rejection cuts are the same for all three event samples. The most sensitive to event kinematics could be the cut on p_T of K^{*0}–meson. The normalized p_T distributions of K^{*0}–meson are shown in Fig. 2c. No disagreement between all three samples of events is observed. It should be noted, that the presented inclusive one particle distributions depend mainly on the B–meson production inclusive spectra and acceptance of the detector.

The particle distributions in B–meson c.m.s. could be more sensitive to the decay form factors. The dilepton mass distributions for events of three samples are presented in Fig. 2d. In this figure all distributions are normalized to unity. The relative differencies in dilepton mass distributions could be observed. The peak at small q^2 is observed in the samples with decays with implemented matrix elements, while in the simplest case of PYTHIA version, the distribution is approximately flat at small q^2. With the IGSW2 parametrization the peak is more pronounced than with the GI parametrization.

In Fig. 3 the same dilepton mass distributions are normalized in accordance with predicted branching ratios. The differencies between the predicted spectra are more clear.

The expected signal event numbers for one year (10^{-7} sec.) LHC run at low luminosity are presented in Table IV. The cross-sections for background events are calculated by renormalizing the background estimates, obtained in [6].

4. Studying the forward-backward asymmetry with ATLAS

As it was pointed out in [6], two important distributions for $B_d^0 \to K^{*0}\mu^+\mu^-$ decay mode can be investigated in experiment:

1) Invariant dilepton mass distribution $d\Gamma/d\hat{s}$ and

2) Forward–backward (FB) charge asymmetry $A_{FB}(\hat{s})$, defined by equation:

$$A_{FB}(\hat{s}) = \frac{\int\limits_0^1 \frac{d^2\Gamma}{d\hat{s}\,d\cos(\theta)} d\cos(\theta) - \int\limits_{-1}^0 \frac{d^2\Gamma}{d\hat{s}\,d\cos(\theta)} d\cos(\theta)}{\int\limits_0^1 \frac{d^2\Gamma}{d\hat{s}\,d\cos(\theta)} d\cos(\theta) + \int\limits_{-1}^0 \frac{d^2\Gamma}{d\hat{s}\,d\cos(\theta)} d\cos(\theta)}, \tag{3}$$

where θ–is the angle between the l^+ and B–meson direction in the rest frame of the lepton pair, $\hat{s} = q^2/M_B^2$.

The differential A_{FB} (Fig. 1b) has some clearly seen regions dominated by the ψ and ψ' resonances. The resonance contributions do not carry the interesting information on the SD effects and should be excluded from the analysis. It is convenient to isolate the following $\hat{s}$–intervals:

1) low $\hat{s}$–range $\hat{s}_{min} < \hat{s} < 0.33$, where $\hat{s}_{min} = 4m_l^2/M_B^2$,

2) high $\hat{s}$–range $0.55 < \hat{s} < \hat{s}_{max}$, where $\hat{s}_{max} = (M_B - M_{K^*})^2/M_B^2$.

Besides, one can see in Fig. 1 a that the asymmetry predicted in the SM, changes its sign in the first $\hat{s}$–range and its average value is close to zero. So, it is reasonable to measure the asymmetry in the intervals $\hat{s}_{min} < \hat{s} < 0.14$ and $0.14 < \hat{s} < 0.33$ separately. The event numbers in each of the three $\hat{s}$–ranges are shown in Table V.

Table V presents also theoretical predictions on A_{FB} in the framework different models for three $\hat{s}$–ranges (were $\hat{s}_1$ and $\hat{s}_2$ are the boundaries of the region). They were calculated according to the following expression:

$$< A_{FB} >_{[\hat{s}_1,\hat{s}_2]} = \frac{< N_F >_{[\hat{s}_1,\hat{s}_2]} - < N_B >_{[\hat{s}_1,\hat{s}_2]}}{< N_F >_{[\hat{s}_1,\hat{s}_2]} + < N_B >_{[\hat{s}_1,\hat{s}_2]}} \tag{4}$$

where $< N_F >_{[\hat{s}_1,\hat{s}_2]}$ and $< N_B >_{[\hat{s}_1,\hat{s}_2]}$ are the numbers of positive leptons moving in forward and backward directions in comparison with B–meson vector correspondingly. They are defined by the next expressions:

$$< N_F >_{[\hat{s}_1,\hat{s}_2]} \sim \int\limits_{\hat{s}_1}^{\hat{s}_2} [\beta_V(\hat{s}) + 3\hat{s}\phi^{1/2}R_1(\hat{s})]d\hat{s}, \qquad < N_B >_{[\hat{s}_1,\hat{s}_2]} \sim \int\limits_{\hat{s}_1}^{\hat{s}_2} [\beta_V(\hat{s}) - 3\hat{s}\phi^{1/2}R_1(\hat{s})]d\hat{s},$$

$$\beta_V(\hat{s}) = 2\phi\hat{s}|G(q^2)|^2 + \left[2\hat{s} + \frac{(1-k-\hat{s})^2}{4k}\right]|F(q^2)|^2 + \frac{\phi^2}{4k}|H_+(q^2)|^2 - 2\frac{\phi}{4k}(\hat{s}-1+k)R(q^2).$$

where the values $|G(q^2)|^2$, $|F(q^2)|^2$, $|H_+(q^2)|^2$, $R(q^2)$ and $R_1(q^2)$ are defined in [8], $k = (M_{K^*}/M_B)^2$, $\phi = \hat{s}^2 + k^2 + 1 - 2\hat{s} - 2k - 2\hat{s}k$. One can see from Table V that the SM and MSSM predictions for both types of form factors are in a good agreement at $\hat{s} \geq 0.55$. At other regions of $\hat{s}$ there are some probabilities to separate these SM and MSSM if the accuracy of asymmetry measurement would be enough.

The expected parts of events in the different $\hat{s}$–regions s for the GI and ISGW2 parametrisations are shown in Table VI.

Let us estimate the lower limits of asymmetry in these three $\hat{s}$–regions after 3 year LHC run at low luminosity in the worst case (the ISGW2 form factor parametrization predicted the lowest value of cross-section). Studying the dimuon mass spectrum for this case we can expect $N_s = 1323$ signal and $N_{BG} = 552$ background events in the $\hat{s}_{min} < \hat{s} < 0.14$ region. The asymmetry

$$< A_{FB} >_{[\hat{s}_1,\hat{s}_2],mean} = \frac{< N_F >_{[\hat{s}_1,\hat{s}_2]} - < N_B >_{[\hat{s}_1,\hat{s}_2]}}{< N_F >_{[\hat{s}_1,\hat{s}_2]} + < N_B >_{[\hat{s}_1,\hat{s}_2]} + N_{BG}} = \frac{\Delta N}{N_s + N_{BG}} \tag{5}$$

can be reliably measured if the ΔN would exceed 2σ. So, measured asymmetry $\mid A_{mean} \mid$ would be of 0.046 and corresponding real value $\mid A_{real} \mid = \Delta N/N_s$ of 0.065. It means that in this $\hat{s}$–region the asymmetry may be measured only if it would be greater than 7 %. The same estimations show that in the $0.14 < \hat{s} < 0.33$ range the lower limit for measurement of the real asymmetry is 0.060. The obtained estimations for the ISGW2 and GI parametrizations are presented in Table VII.

It is obvious that the expected lower limit on the asymmetry measurements of 10 % will alow one to reject a very large class of MSSM with $R_{7\gamma} < 0$ if a measured asymmetry occured to be positive in the interval $\hat{s}_{min} < \hat{s} < 0.14$.

In a more complicate case if the measured asymmetry is found to have a positive sign in the first $\hat{s}$-region, the MSSM predictions are beyond the expected accuracy (smaller than 9 %). Fortunately, the measurements in the second $\hat{s}$-range will allow us to conclude more definitely on the presence of the new physics. In the high $\hat{s}$–region the SM and MSSM are not distinguishable. The measurements in this region can can be used for the general analysis of the experimental sensitivity.

5. Conclusions

We have analyzed a possibility of an experimental study of rare $B \to K^*\mu^+\mu^-$ decays with the ATLAS detector at LHC. Our main conclusions are as follows:

1 The uncertainty in the theoretical predictions for the transition form factors strongly influence the dimuon q^2–distributions and the branching ratio, but remain practically unaffected the single-particle muon P_T-distributions and forward-backward lepton differential asymmetries.

2 It will be possible to measure $BR(B \to K^*\mu^+\mu^-)$ with high accuracy at ATLAS. The expected $Signal/BG$ ratio is found to be $2 \div 4$ depending on the different parametrizations of the transition form factors.

3 Even in the worst case, the $Signal/BG$ ratio equal 2, it will be possible to measure the forward-backward asymmetry with an accuracy of 10% after a 3 year LHC run at low luminosity. Such accuracy is sufficient to discriminate between the SM and some variants of the MSSM.

Acknowledgements

We are grateful to S. Baranov for useful discussions.

---

[1] B.Grinstein, M. B.Wise, and M.J.Savage, Nucl.Phys. B319 (1989) 271
[2] A.Buras and M. Münz, Phys.Rev. D52 (1995) 186.
[3] D.Melikhov, N.Nikitin and S.Simula, Phys. Lett. B410 (1997) 290
[4] A.Ali, C.Greub and T.Mannel, preprint DESY 93-016.
[5] A.Ali, preprint DESY 96-106, hep-ph/9606324.
[6] D.Melikhov, F.Rizatdinova, S.Sivoklokov and L.Smirnova, ATLAS Internal Note, 1994.
D.Melikhov, F.Rizatdinova and L.Smirnova, ATLAS Internal Note PHYS-NO-083, 2 April 1996.
[7] P.Cho, M.Misiak and D.Wyler, Phys. Rev. D54 (1996) 3329; J.L.Hewett, J.D.Wells, Phys.Rev. D55, (1997) 5549.
[8] D.Melikhov, N.Nikitin and S.Simula, Phys. Rev. D57 (1998) 6814.

TABLE I. Non-resonance branching ratios of the decays $B \to K(K^*)l^+l^-$. We present results for the two sets of the form factors from ref [3].

Ref.	$\mathcal{BR}(B \to K\mu^+\mu^-)$	$\mathcal{BR}(B \to K^* e^+e^-)$	$\mathcal{BR}(B \to K^*\mu^+\mu^-)$
Set 1	3.2×10^{-7}	0.8×10^{-6}	0.7×10^{-6}
Set 2	5.3×10^{-7}	1.9×10^{-6}	1.4×10^{-6}
average value [3]	$(4.2 \pm 0.9) \times 10^{-7}$	$(1.4 \pm 0.5) \times 10^{-6}$	$(1.0 \pm 0.4) \times 10^{-6}$
A. Ali et al. [4]	6×10^{-7}	5.6×10^{-6}	2.9×10^{-6}
A. Ali [5]	$(4.0 \pm 1.5) \times 10^{-7}$	$(2.3 \pm 0.9) \times 10^{-6}$	$(1.5 \pm 0.6) \times 10^{-6}$

TABLE II. Average transverse momenta of decay particles.

	PYTHIA	GI	ISGW2
$\langle p^{\mu}_{Tmin} \rangle$	7.66 ± 0.13	7.6 ± 0.07	7.58 ± 0.07
$\langle p^{\mu}_{Tmax} \rangle$	12.55 ± 0.25	12.5 ± 0.15	12.46 ± 0.15
$\langle p_T \rangle_{K^{*0}}$	8.63 ± 0.25	7.9 ± 0.14	7.95 ± 0.14

TABLE III. Analysis cuts for $B^0_d \to K^{*0}\mu^+\mu^-$ events. Br=Br($B^0_d \to K^{*0}\mu^+\mu^-$).

Cuts	PYTHIA	GI	ISGW2
$4 < M_{eff}(K^*\mu\mu) < 7\ GeV/c^2$, $p^{\mu}_{T1} > 5$ GeV/c, $\mid \eta \mid < 2.5$ $p^{\mu}_{T2} > 5$ GeV/c, $\mid \eta \mid < 2.5$	100%	100%	100%
Decay length of $B^0_d > 1.0$ mm Decay length of $K^{*0} > 1.0$ mm $\chi^2/NDF < 3$	47 %	48 %	48.6 %
Angle between p_T of B^0_d and line joining primary and B^0_d-decay vertices $\alpha < 3°$	42%	43%	43.3 %
$n_{ch}(p_T > 1\text{GeV/c}) = 0$ in cone $\theta < 9°$	21.5 %	25 %	25.5 %
$M^{eff}_{\mu\mu} \notin J/\psi$, $M^{eff}_{\mu\mu} \notin \psi'$	17.6 %	22 %	21.3 %
p_T of $K^{*0} > 5$ GeV/c	13 %	16 %	15.5 %
$5.2 < M_{eff} < 5.32$ GeV/c	11.5 %	13 %	12.4 %
$\epsilon(\mu\mu) = 0.8^2$	7.4 %	8.3 %	7.9 %

TABLE IV. Cross-sections for different matrix elements and background after cuts.

Model	Cross-section	Number of events for 1 year low luminosity run
PYTHIA	$0.18 \cdot \text{Br}_{\text{Ali [5]}}\ \mu$b	2700
ISGW2	$0.18 \cdot \text{Br}_{\text{ISGW2}}\ \mu$b	1272
GI	$0.19 \cdot \text{Br}_{\text{GI}}\ \mu$b	2672
BG	$6.3 \cdot 10^{-5}$ nb	630

TABLE V. Theoretical prediction for expected asymmetries $< A_{FB} >_{[\hat{s}_1,\hat{s}_2]}$ in the SM and MSSM ($\hat{s}_{min} = 4m_l^2/M_B^2$, where m_l is lepton mass and $\hat{s}_{max} = (M_B - M_{K^*})^2/M_B^2$).

Interval of the $\hat{s} = q^2/M_B^2$				$\hat{s}_{min} \div 0.14$	$0.14 \div 0.33$	$0.55 \div \hat{s}_{max}$
SM	ISGW2			0.10	−0.14	−0.29
	GI			0.08	−0.13	−0.32
MSSM		ISGW2	$R_{7\gamma} = 0.4$	0.05	−0.20	−0.30
			$R_{7\gamma} = 1.2$	0.11	−0.13	−0.29
			$R_{7\gamma} = -2.4$	−0.18	−0.33	−0.32
			$R_{7\gamma} = -4.2$	−0.17	−0.35	−0.33
		GI	$R_{7\gamma} = 0.4$	0.04	−0.18	−0.33
			$R_{7\gamma} = 1.2$	0.08	−0.12	−0.31
			$R_{7\gamma} = -2.4$	−0.15	−0.29	−0.35
			$R_{7\gamma} = -4.2$	−0.15	−0.32	−0.36

TABLE VI. Expected percents of events in the different $\hat{s} = q^2/M_B^2$ regions ($\hat{s}_{min} = 4m_l^2/M_B^2$, where m_l is lepton mass and $\hat{s}_{max} = (M_B - M_{K^*})^2/M_B^2$).

interval	$\hat{s}_{min} \div 0.14$	$0.14 \div 0.33$	$0.55 \div \hat{s}_{max}$
ISGW2	23 %	28.3 %	15 %
GI	14.4 %	23 %	24 %

TABLE VII. Expected absolute lower limits for asymmetry measurements after 3 years LHC run at low luminosity ($\hat{s}_{min} = 4m_l^2/M_B^2$, where m_l is lepton mass and $\hat{s}_{max} = (M_B - M_{K^*})^2/M_B^2$).

interval	$\hat{s}_{min} \div 0.14$	$0.14 \div 0.33$	$0.55 \div \hat{s}_{max}$
ISGW2	0.065	0.060	0.090
GI	0.053	0.041	0.040

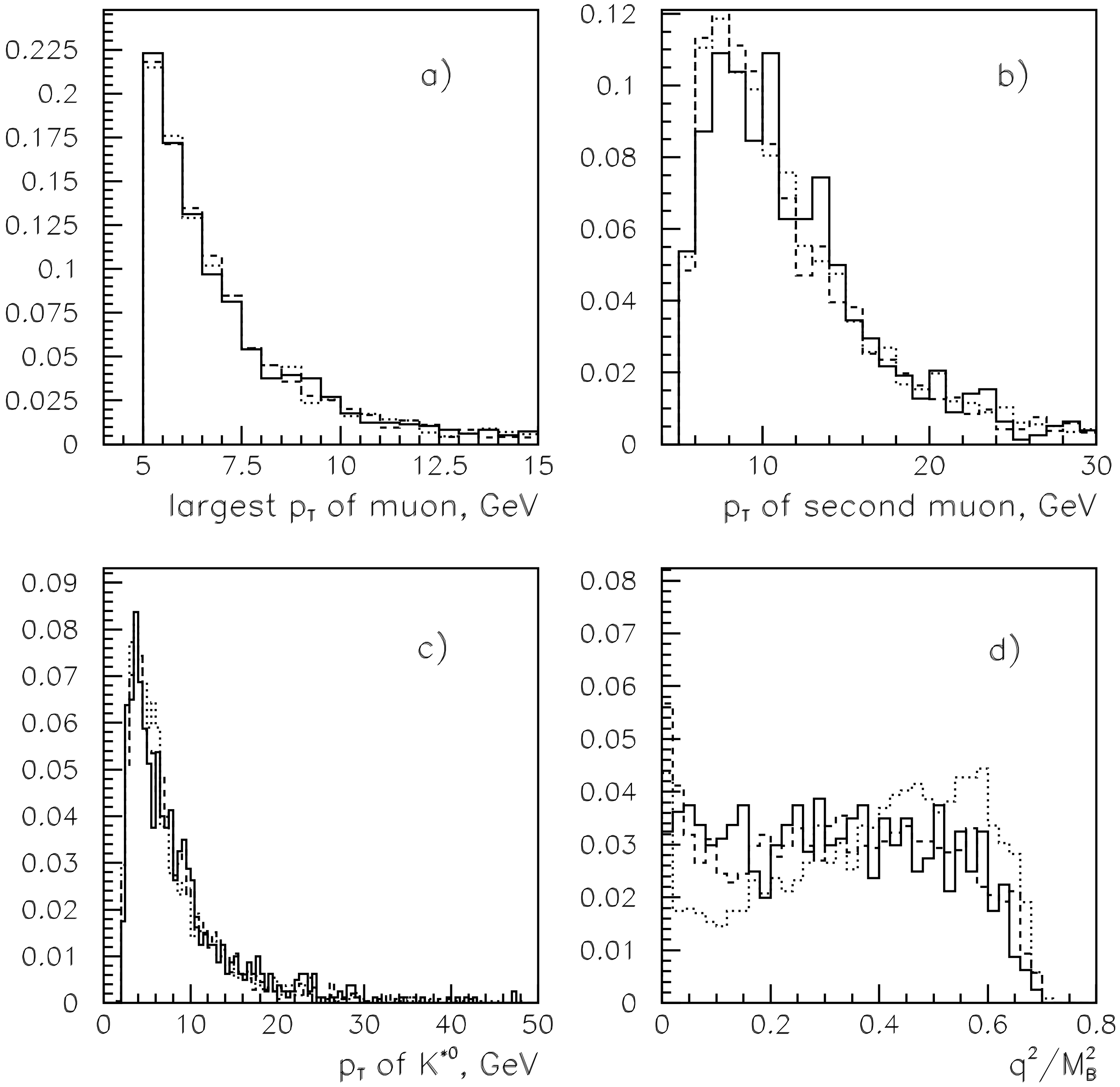

FIG. 1. The characteristics for decay $B_d^0 \to K^{*0}\mu^+\mu^-$ for different matrix elements. Solid line corresponds to PYTHIA matrix element predictions, dashed – GI parameters (Set 2) and dotted – ISGW2 parameters (Set 1). For more detailes see the text in Sec. 3.

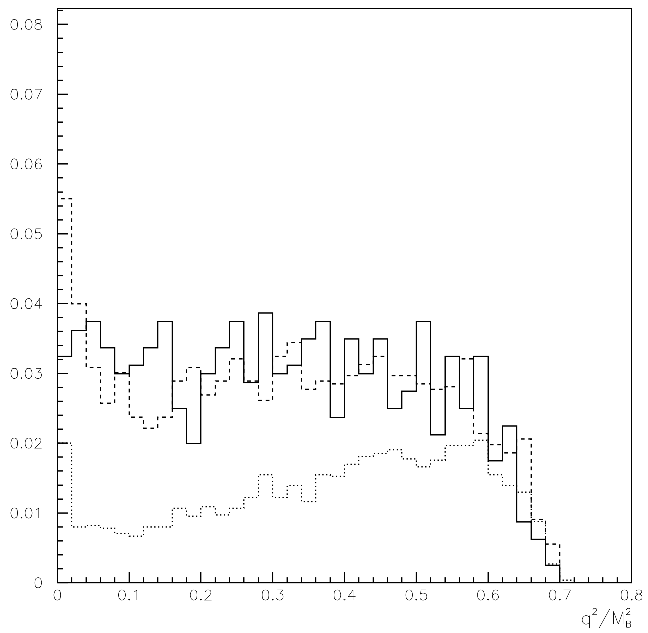

FIG. 2. Invariant dilepton mass distribution, normalised on the cross section corresponding PYTHIA calculation. Solid line corresponds to PYTHIA matrix element predictions, dashed – to GI parameters (Set 2) and dotted – to ISGW2 parameters (Set 1). For more detailes see the text in the end of Sec. 3.

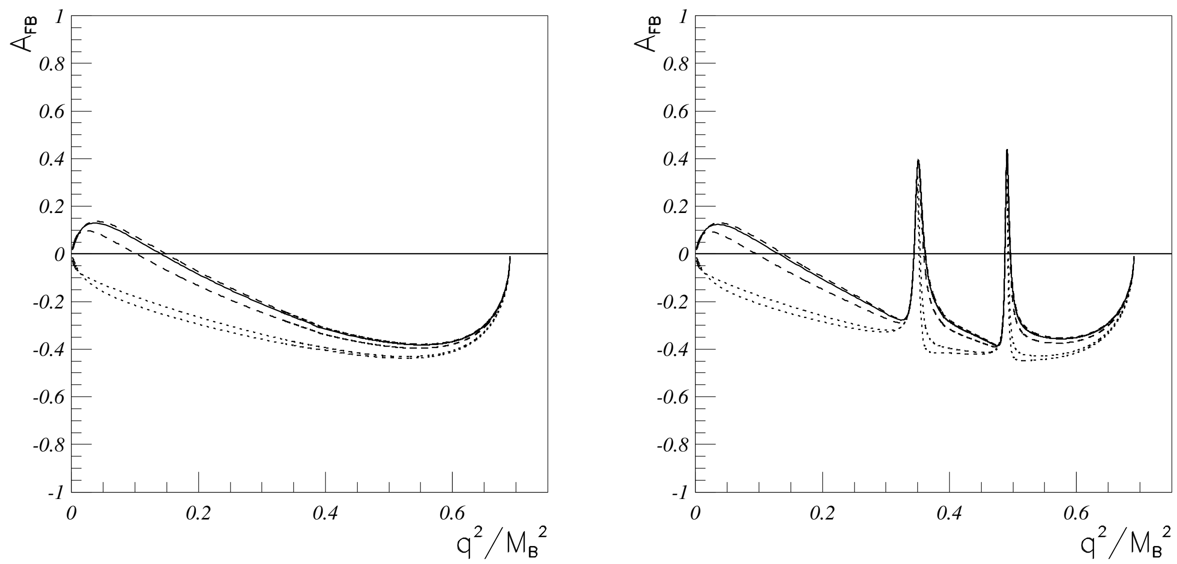

FIG. 3. Forward–backward asymmetry A_{FB} for the decay $B \to K^* \mu^+ \mu^-$ for the GI parametrisation: (a) non–resonant and (b) the sum of non–resonant and resonant contributions. Solid - SM, dashed - MSSM for $1.2 > R_{7\gamma} > 0.4$, dotted - MSSM for $-2.4 > R_{7\gamma} > -4.2$, where $R_{7\gamma} = C_{7\gamma}(M_W)_{MSSM}/C_{7\gamma}(M_W)_{SM}$ (see text in Sec.2).